The Plant Cell, Vol. 10, 1107–1120, July 1998, www.plantcell.org © 1998 American Society of Plant Physiologists

Changing Patterns of Localization of the Tobacco Mosaic Virus Movement Protein and Replicase to the Endoplasmic Reticulum and Microtubules during Infection

Manfred Heinlein,[a,1] Hal S. Padgett,[a] J. Scott Gens,[b] Barbara G. Pickard,[b] Steven J. Casper,[a,2] Bernard L. Epel,[c] and Roger N. Beachy[a,3]

[a]Division of Plant Biology, BCC 206, Department of Cell Biology, Scripps Research Institute, 10550 North Torrey Pines Road, La Jolla, California 92037

[b]Biology Department, Washington University, St. Louis, Missouri 63130-4899

[c]Department of Plant Sciences, Tel Aviv University, Tel Aviv 69978, Israel

Tobacco mosaic virus (TMV) derivatives that encode movement protein (MP) as a fusion to the green fluorescent protein (MP:GFP) were used in combination with antibody staining to identify host cell components to which MP and replicase accumulate in cells of infected *Nicotiana benthamiana* leaves and in infected BY-2 protoplasts. MP:GFP and replicase colocalized to the endoplasmic reticulum (ER; especially the cortical ER) and were present in large, irregularly shaped, ER-derived structures that may represent "viral factories." The ER-derived structures required an intact cytoskeleton, and microtubules appeared to redistribute MP:GFP from these sites during late stages of infection. In leaves, MP:GFP accumulated in plasmodesmata, whereas in protoplasts, the MP:GFP was targeted to distinct, punctate sites near the plasma membrane. Treating protoplasts with cytochalasin D and brefeldin A at the time of inoculation prevented the accumulation of MP:GFP at these sites. It is proposed that the punctate sites anchor the cortical ER to plasma membrane and are related to sites at which plasmodesmata form in walled cells. Hairlike structures containing MP:GFP appeared on the surface of some of the infected protoplasts and are reminiscent of similar structures induced by other plant viruses. We present a model that postulates the role of the ER and cytoskeleton in targeting the MP and viral ribonucleoprotein from sites of virus synthesis to the plasmodesmata through which infection is spread.

INTRODUCTION

Most plant viruses encode one or more proteins that are required to achieve local and systemic invasion of the host. These so-called movement proteins (MPs) enable viruses to exploit plasmodesmata, the gated, plasma membrane–lined channels that provide symplastic continuity between adjacent cells and through which plant cells communicate (Epel, 1994; Lucas and Gilbertson, 1994; Fenczik et al., 1995).

Pioneering studies of MP functions were performed with the MP of tobacco mosaic virus (TMV) (Deom et al., 1987; Meshi et al., 1987). In infected tobacco plants as well as in transgenic plants, the MP accumulates in plasmodesmata and increases their size exclusion limit (Tomenius et al., 1987; Wolf et al., 1989; Atkins et al., 1991a; Ding et al., 1992; Moore et al., 1992; Oparka et al., 1997). The protein also binds single-stranded nucleic acids in vitro, resulting in unfolded and elongated protein–nucleic acid complexes. This observation led to the hypothesis that the virus moves from cell to cell in the form of a viral ribonucleoprotein complex (vRNP) that in size and structure is compatible with the modified plasmodesmata (Citovsky et al., 1990, 1992).

Although it is evident that the MP and vRNP must enlist cytoplasmic structures to aid transfer from their site of synthesis to the plasmodesmata, little is known about the nature of these components and about the targeting mechanism per se. F-actin and microtubules were proposed as targeting systems for MP (Heinlein et al., 1995; McLean et al., 1995; Carrington et al., 1996) because each can participate in translocation of vesicles, organelles, proteins, and even mRNA (Wilhelm and Vale, 1993; Cole and Lippincott-Schwartz, 1995; Johnston, 1995). Recent studies showed that in tobacco BY-2 protoplasts infected by wild-type TMV or by a modified TMV encoding an MP–green fluorescent protein (MP:GFP) fusion protein, the MP and MP:GFP associated with cortical microtubules (Heinlein et al., 1995; McLean et al., 1995) and with actin filaments (McLean et al., 1995). McLean et al. (1995) also reported that TMV MP can interact with tubulin and F-actin in vitro. Other studies suggest an association of actin with plasmodesmata (White et al., 1994; Ding

[1]Current address: Friedrich Miescher-Institut, P.O. Box 2543, CH-4002 Basel, Switzerland.

[2]Current address: Biology Department, Washington University, St. Louis, MO 63130-4899.

[3]To whom correspondence should be addressed. E-mail beachy@scripps.edu; fax 619-784-2994.

and Kwon, 1996), and it was proposed that microtubules may mediate vRNP transport from membrane sites of synthesis to actin filaments, which deliver the viral complexes to plasmodesmata (Zambryski, 1995; Carrington et al., 1996).

Analysis of fluorescent infection sites found on leaves of *Nicotiana benthamiana* as well as analysis of *N. tabacum* infected with another tobamovirus, Ob, revealed that association of the MP with cellular elements is more complex than simple association of MP with microtubules and actin filaments. In infected leaf cells, MP:GFP fluorescence was detected not only in regions within the cell wall presumed to be plasmodesmata and as filamentous structures presumed to be microtubules but also in irregularly shaped bodies of unknown origin (Epel et al., 1996; Padgett et al., 1996). Moreover, although plasmodesmata were labeled throughout the infection site, accumulation in the other structures was transient and differed between cells at different radial positions within the infection site (Padgett et al., 1996).

The purposes of the present study were (1) to use the type member of the tobamovirus group, TMV, to compare the distribution of MP:GFP produced during infection of tobacco BY-2 protoplasts with the patterns of subcellular accumulation in TMV-infected *N. benthamiana* leaves and (2) to use antibodies to label infected protoplasts to establish the spatial relationship between MP:GFP, TMV replicase, microtubules, and other cellular components. This study revealed similar distributions of MP:GFP between plant cells and protoplasts during the course of infection. MP:GFP and viral replicase colocalized to the cortical endoplasmic reticulum (ER) and to irregularly shaped structures that are apparently derived from ER and that may represent sites of virus replication. The results of studies with the inhibitors cytochalasin D (Cyt D), oryzalin, and brefeldin A (BFA) support the role of microtubules, actin filaments, and the ER in the targeting and accumulation of MP:GFP in protoplasts. Considering that actin is associated with the ER and that the ER and microtubules can be close together (Quader et al., 1987; Hepler et al., 1990) or closely associated (Lancelle et al., 1987; Reuzeau et al., 1997a, 1997b), we propose a model to describe how the ER and the cytoskeleton carry the MP and vRNP from their sites of synthesis to the plasmodesmata through which infection is spread.

RESULTS

Accumulation of MP:GFP in Protoplasts and Leaves Infected by TMV–MP:GFP

Accumulation of MP:GFP in Infected Protoplasts

Protoplasts were isolated from BY-2 cell cultures and infected with transcripts of cloned cDNAs of TMV that encode the MP:GFP fusion protein in a construct termed TMV–MP:GFP (previously referred to as TMV-M:GfusBr; Heinlein et al., 1995; Oparka et al., 1997). A representative time course of accumulation and subsequent loss of MP:GFP fluorescence is shown in Figures 1A and 1B and is similar to that ob-

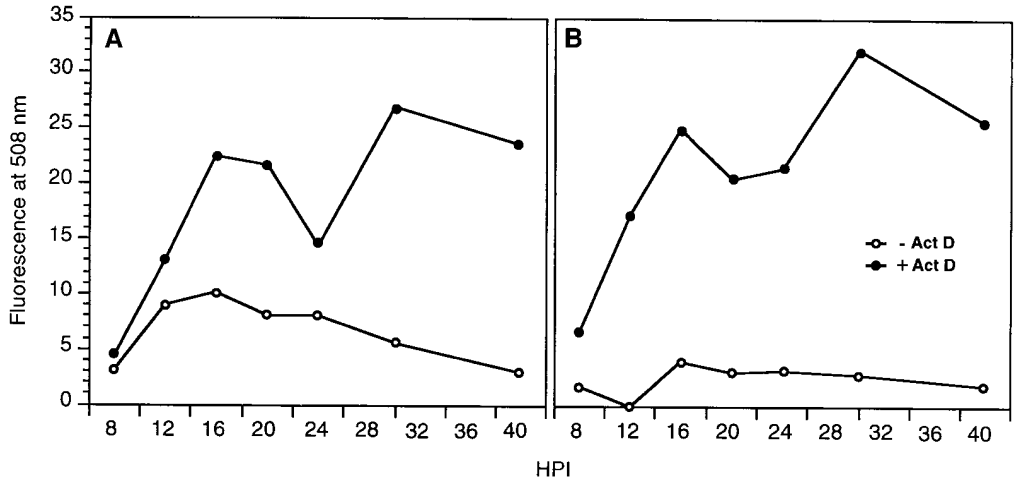

Figure 1. MP:GFP Accumulation in BY-2 Protoplasts Detected by Fluorescence Emission at Given Time Points after Inoculation in the Presence or Absence of 30 μg/mL Act D.

(A) Protoplasts infected with TMV–MP:GFP.

(B) Protoplasts infected with TMV–MP:GFP–CP.

MP:GFP accumulated until 16 HPI and then decreased to a lower level. Act D in the culture medium caused much higher MP:GFP levels, which is consistent with strongly increased MP expression in the presence of Act D (Blum et al., 1989).

served in protoplasts infected with another tobamovirus, ObM:Gfus (Epel et al., 1996; Padgett et al., 1996). In these studies, MP:GFP fluorescence increased until ~16 hr postinfection (HPI) and then decreased to a lower level through 40 HPI.

When fixed protoplasts harvested at 8, 12, 16, 20, 24, and 30 HPI were examined by fluorescence microscopy, significant differences in the accumulation and subcellular localization of the MP:GFP were observed. The sequence describing the accumulation of MP:GFP in various structures shown in Figure 2 was established by identifying the time at which particular fluorescent patterns first appeared as well as by determining the frequency of each pattern at successive times after infection (Figures 3A and 3B). Together, the observations suggest the following sequence of events. At 7 to 8 HPI, MP:GFP is seen in peripheral punctate structures that are observed through 30 HPI (Figures 2A and 2F). Between 8 and 12 HPI, MP:GFP accumulates in small irregularly shaped structures (Figure 2B), and between 12 and 20 HPI, these grow in size, or coalesce, to form larger and fewer structures (Figure 2C). The next stage of infection (16 to 24 HPI) is characterized by the association of MP:GFP with filaments (previously identified as association of MP:GFP with microtubules; Heinlein et al., 1995) that apparently interlink the irregular structures (Figure 2D), which at this time begin to decrease in size. Between 20 and 30 HPI, MP:GFP, in most protoplasts, is associated only with microtubules (Figure 2E) and the peripheral puncta. With increasing time, MP:GFP levels continue to decrease, and MP:GFP is restricted to the peripheral punctae that persisted throughout infection and to a haze of fluorescence within the cytoplasm (Figure 2F). This haze may represent degradation of MP:GFP or a soluble form of the fusion protein. Throughout the time course, a low but increasing percentage of protoplasts (up to 15%) developed plasma membrane protrusions labeled with MP:GFP (Figures 2G and 3).

The virus construct used in these studies did not contain the coat protein (CP) gene. Based on the work of Culver et al. (1993), it was expected that infection by a virus construct that produced CP in addition to MP:GFP, that is, TMV–MP:GFP–CP (referred to as TMV-MfCP in Oparka et al. [1997]), would result in decreased synthesis and accumulation of MP:GFP. This was shown to be the case in infected protoplasts (Figure 1); nevertheless, each of the fluorescent structures observed in cells infected by TMV–MP:GFP were also observed in cells infected by TMV–MP:GFP–CP, although the percentage of cells that contained fluorescent irregular structures and microtubules was significantly decreased (Figure 3). However, despite the low level of MP:GFP in these structures, most protoplasts exhibited equivalent numbers of fluorescent peripheral punctae. Likewise, the appearance of MP:GFP–containing plasma membrane protrusions was approximately the same in protoplasts infected with either virus (Figure 3).

It is possible to significantly increase gene expression from the subgenomic virus promoter that leads to expression of MP by adding actinomycin D (Act D) to the medium (Blum et al., 1989). When Act D was added to 30 μg/mL to cultures of protoplasts inoculated with TMV–MP:GFP or TMV–MP:GFP–CP, there was a dramatic increase in the amount of MP:GFP fluorescence (Figure 1). Infected protoplasts treated with Act D accumulated proportionally more MP:GFP in the irregular fluorescent structures than in other structures (e.g., fluorescent punctate structures, microtubules, and plasma membrane protrusions; data not shown).

Accumulation Pattern of MP:GFP in Infection Sites on Leaves

Leaves of *N. benthamiana* that were inoculated with TMV–MP:GFP produced fluorescent rings that enlarged in diameter with time (Heinlein et al., 1995; Figure 2H), similar to those reported for the tobamovirus ObM:GfusBr on leaves of *N. tabacum* (Padgett et al., 1996). When cells were examined by fluorescence microscopy from the outer (leading) edge of the expanding ring to the center of the ring, patterns of subcellular accumulation of MP:GFP similar to those in infected BY-2 protoplasts were observed. In cells at the outer edge, which presumably represent newly infected cells, MP:GFP was associated with punctate structures in cell walls (Figure 2I). Punctate fluorescence was seen in cell walls throughout the infection site and previously was shown to be associated with plasmodesmata (Oparka et al., 1997). Moving progressively toward the center of the ring, MP:GFP was associated with small and large irregularly shaped fluorescent structures (Figures 2J and 2K), with irregular structures and filaments (microtubules) (Figure 2L), and with fluorescent filaments (microtubules) alone (Figure 2M). In the center, MP:GFP was exclusively associated with plasmodesmata (Figure 2N).

When *N. benthamiana* was infected with TMV–MP:GFP–CP, the accumulation of MP:GFP in infection sites was, as predicted, less than that produced by TMV–MP:GFP (J. Szecsi, X.S. Ding, C.O. Lim, M. Bendahmane, M.J. Cho, R.S. Nelson, and R.N. Beachy, submitted manuscript). As in protoplasts, the number of cells containing the irregularly shaped bodies and filaments containing MP:GFP was low, presumably because the amount of MP:GFP produced by virus that produces CP is significantly less than that from virus that does not produce CP. Nevertheless, in infection sites produced by TMV–MP:GFP–CP, fluorescence was always observed in plasmodesmata.

Analysis of Subcellular Accumulation of MP:GFP

MP:GFP in Punctate Structures at the Periphery of Protoplasts

Green fluorescent punctate structures are readily visible when the curved upper surface of protoplasts is in the plane

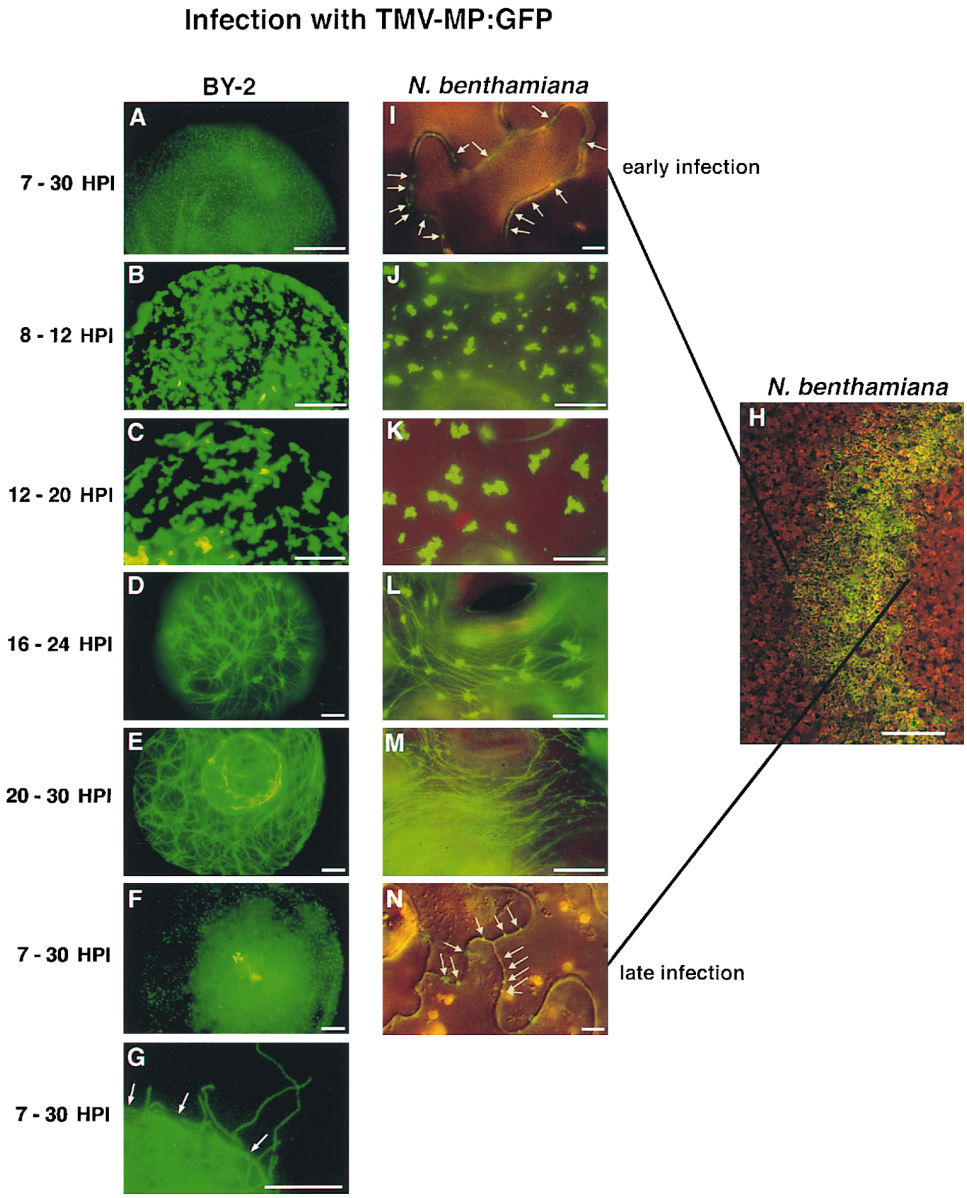

Figure 2. Accumulation and Distribution of MP:GFP in BY-2 Protoplasts and in Cells across Infection Sites on *N. benthamiana* Leaves Infected with TMV–MP:GFP.

(A) to **(G)** Accumulation and distribution of fluorescent MP:GFP in the population of infected tobacco BY-2 protoplasts at given times after inoculation. In **(A)**, MP:GFP is associated with peripheral punctate structures throughout the time course of infection (7 to 30 HPI). In **(B)**, MP:GFP becomes detectably associated with small irregular fluorescent structures at 8 to 12 HPI. In **(C)**, the irregular structures increase in size between 12 and 20 HPI. In **(D)**, the irregular fluorescent structures decrease in size and appear to be interlinked with filaments (microtubules) at 16 to 24 HPI. In **(E)**, MP:GFP between 20 and 30 HPI is no longer associated with irregular structures but is detectably associated only with filaments (microtubules) (and peripheral punctate structures as in **[A]** that are not focused). At late stages of infection (30 HPI), green fluorescence is detectable only with punctate structures and as a background fluorescence **(F)**. Protoplasts exhibiting plasma membrane protrusions containing MP:GFP are seen throughout the infection. Arrows indicate location of the plasma membrane **(G)**. Bars = 10 μm.
(H) Sector of a green fluorescent ring-shaped infection site on an *N. benthamiana* leaf. Bar = 0.5 mm.
(I) to **(N)** Subcellular distribution of MP:GFP in cells across an infection site. At the leading edge of the infection and throughout the infection site, MP:GFP is associated with punctate sites in the cell walls (arrows) that mark the location of plasmodesmata **(I)**. In **(J)**, MP:GFP is associated with small irregular fluorescent structures near the infection front. In **(K)**, MP:GFP is associated with large irregular structures within the region of highest fluorescence in the ring. In **(L)**, MP:GFP is associated with small irregular fluorescent structures, with filaments (microtubules) toward the

of focus (Figure 4A, left), and they appear to be tightly appressed to the cell periphery when the center of the protoplasts is in the plane of focus (Figure 4A, right). Similar structures were also detected in protoplasts infected with wild-type TMV after staining with the anti-MP antibody (data not shown).

In some cells, the punctae appear to be arranged in rows (Figure 4B, left) and sometimes occur in the vicinity of microtubules (Figure 4B, right). To locate more accurately the punctate structures, we used wide-field computational optical-sectioning microscopy. In this study, 0.45-μm optical sections of infected protoplasts were obtained with a pixel size of 0.22 × 0.22 μm, and fluorescence was restored toward the sites of emission, as described previously (Gens et al., 1996). Stereopairs computationally created from the data are presented in Figures 4C and 4D. As shown in these figures, the MP:GFP–containing punctate structures are present on the outer surface of the cell and apparently are connected by a fine, MP:GFP–associated cortical network.

The fluorescence of the MP:GFP associated with the cortical network sometimes was sufficiently strong for detection by conventional fluorescence microscopy (Figure 4E, left). The pattern of this network is similar to the reticulate pattern of the cortical ER that was visualized in protoplasts after staining with $DiOC_6$, which is known to stain the ER (Figure 4E, right). To confirm that the MP:GFP is associated with the ER, we stained infected protoplasts with antibodies against immunoglobulin binding protein (BiP), a luminal ER constituent (Fontes et al., 1991; Boston et al., 1996). The pattern of MP:GFP fluorescence (Figure 4F, left) and the pattern of red anti-BiP antibody labeling (Figure 4F, center) are closely comparable, and superposition of the images demonstrates significant overlap between the location of the ER marker BiP and the MP:GFP (Figure 4F, right). Therefore, we conclude that the polygonal network with which MP:GFP associates is the cortical ER. The anti-BiP antibody did not bind detectably to the fluorescent puncta, indicating that either (1) the punctate structures are adjacent to the ER rather than a part of it or (2) the punctate structures may represent a subcompartment of the ER that does not contain sufficient amounts of BiP to be detected or is not accessible to the antibody.

To characterize further the association of MP:GFP with the punctate structures, infected protoplasts were treated with compounds known to affect ER and filamentous actin and tubulin. BFA is a fungal metabolite that affects the endomembrane system and secretory pathways (Satiat-Jeunemaitre and Hawes, 1993; Henderson et al., 1994; Satiat-Jeunemaitre et al., 1996). In both plant and animal cells, BFA disrupts Golgi-based secretion. However, in plant cells, the drug also affects the ER (Driouich et al., 1993; Rutten and Knuiman, 1993; Schindler et al., 1994) and may destroy the network when used in high concentrations (>100 μg/mL) (Henderson et al., 1994). We incubated protoplasts with 50 μg/mL BFA immediately after inoculation with TMV–MP:GFP or TMV–MP:GFP–CP. In nontreated protoplasts, MP:GFP was associated with the punctate sites at 8 HPI (Figure 4G, left), whereas in the treated protoplasts, little or no MP:GFP accumulated in the punctate sites at 8 (Figure 4G, center left), 16, 22, and 30 HPI (data not shown). However, when BFA was added at 8, 12, 16, or 22 HPI, MP:GFP accumulated in the punctate sites equally in treated and nontreated protoplasts.

The microtubule-disrupting herbicide oryzalin (10 μm) (Hugdahl and Morejohn, 1993) did not inhibit accumulation of MP:GFP in punctate structures in infected protoplasts. However, in protoplasts treated with oryzalin from 0 to 30 HPI or between 22 and 30 HPI, the punctate sites containing MP:GFP were noticeably larger than in nontreated protoplasts (Figure 4G, center right), suggesting that microtubules may be involved in the structure of these sites.

Infected protoplasts that were cultured in the presence of 25 μg/mL of Cyt D were characterized by reduced fluorescence of the punctae (Figure 4G, right), indicating that when filamentous actin is disrupted, the accumulation, aggregation, anchoring, or persistence of MP:GFP at these sites may be inhibited.

MP:GFP in Irregularly Shaped Structures

Most of the irregularly shaped fluorescent structures develop from the cortical ER in the outermost periphery of the protoplasts, and fewer are found in the center of the cells (Figures 5A and 5B), sometimes surrounding the nucleus (data not shown). As could be seen in live cells by three-dimensional microscopy, the cortical structures developed immediately interior to microtubules (Figure 5C), which is consistent with the normal spatial distribution of the cortical ER relative to microtubules in plant cells.

The spatial distribution of the irregular, MP:GFP–labeled structures was correlated with location of microtubules by staining fixed cells with anti-tubulin antibody and rhodamine-labeled secondary antibody (Figure 5D). At 16 HPI, the

Figure 2. (continued).

rear of the ring. In **(M)**, MP:GFP is associated with filaments (microtubules) alone that are in a small zone at the trailing edge of the fluorescent infection site. In the center of the ring where MP:GFP accumulation is diminished to very low levels, MP:GFP is associated exclusively with plasmodesmata. Arrows indicate the location of plasmodesmata **(N)**. Bars = 10 μm.

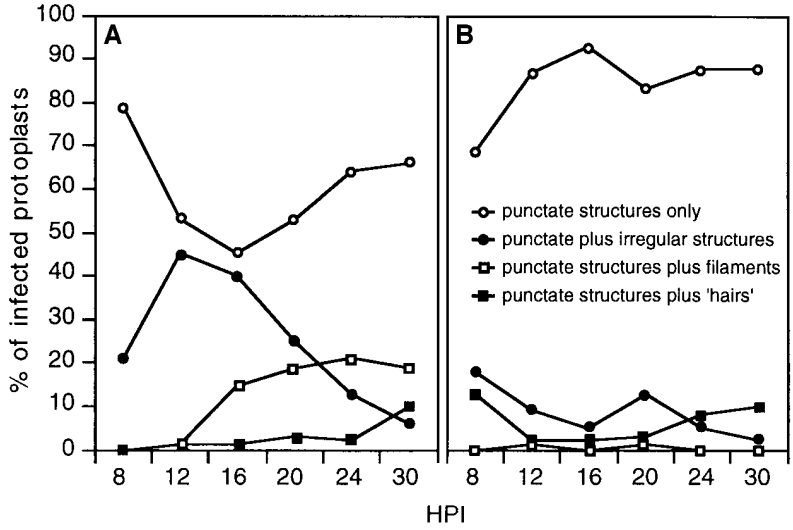

Figure 3. MP:GFP Distribution Patterns in the Protoplast Population at Given Time Points after Inoculation.

(A) Protoplasts infected with TMV–MP:GFP.
(B) Protoplasts infected with TMV–MP:GFP–CP.

MP:GFP–containing structures were closely associated with microtubules, and later in infection (e.g., 20 HPI), when the microtubules were apparently covered with MP:GFP, the ER-associated fluorescent structures often appeared to be dragged apart along the filaments (Figure 5D). This is consistent with the hypothesis that the MP:GFP, either free or in association with material, is redistributed from labeled ER onto microtubules.

Treatment of protoplasts with oryzalin caused the irregular, MP:GFP–containing structures to lose shape and to coalesce (data not shown), suggesting that microtubules may be involved in the spatial separation of these structures. Treatment of infected cells with Cyt D altered the shape of the MP:GFP–containing structures (data not shown), suggesting that actin confers structural support to these structures.

When BFA was added to protoplasts at the time of infection, the accumulation of MP:GFP in the irregular fluorescent structures was inhibited. However, when BFA was added at 8 to 20 HPI and protoplasts were observed at 22 or 30 HPI, there was no apparent effect on MP:GFP accumulation. These data suggest that BFA inhibits the establishment of, or the association of MP:GFP with, these structures but has no influence once the structures are formed.

To determine whether any of the MP:GFP–containing structures represent sites of virus replication, protoplasts were harvested at various times after infection with TMV–MP:GFP or TMV–MP:GFP–CP and were stained with antibody against TMV replicase (Nelson et al., 1993) followed by rhodamine-conjugated secondary antibody. As shown in Figure 5E, the anti-replicase antibody labeled the irregular fluorescent structures. The antibody also labeled the cortical ER, supporting the hypothesis that the irregular structures are ER (data not shown). In contrast, the anti-replicase antibody was not detected using these methods with the fluorescent punctae or with microtubules. These results indicate that ER and irregular fluorescent structures are likely to be sites of virus replication. Similar results were obtained with protoplasts infected with wild-type TMV (data not shown).

MP:GFP–Labeled Filaments

It was shown previously that the MP:GFP fluorescent filaments observed in infected protoplasts result from association of the fusion protein with microtubules and that treatment of infected protoplasts with oryzalin disrupted the filaments, whereas Cyt D had no detectable effect on filaments (Heinlein et al., 1995). When BFA was added at the time of inoculation, the association of MP:GFP with microtubules was inhibited, whereas the drug had no effect when added at 8 HPI or later (data not shown).

Protrusions from the Plasma Membrane of Infected Protoplasts Contain MP:GFP

In a low percentage of cells infected with TMV–MP:GFP or TMV–MP:GFP–CP, fluorescent protrusions were formed on the surface of the protoplasts (Figure 2G). The formation of these plasma membrane protrusions was inhibited in cells treated with BFA. The extracellular protrusions were not

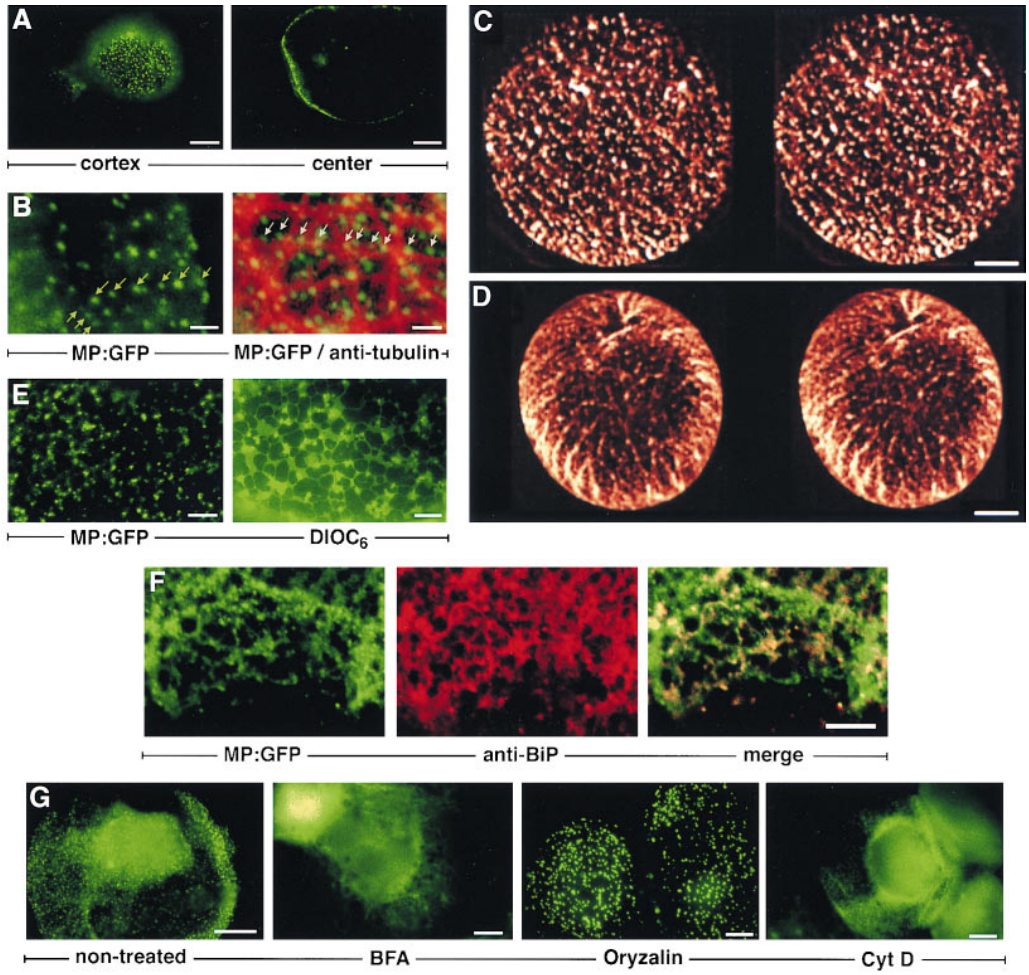

Figure 4. MP:GFP Is Associated with Punctate Structures That Are Located at the Periphery of Infected Protoplasts and Are Associated with Cortical ER.

(A) Fluoromicroscopy of a live protoplast focused on the cortex (left) and the center (right). Bars = 10 μm.

(B) MP:GFP is associated with punctate structures that appear to be arranged in rows (left, arrows) and sometimes are aligned to microtubules (right, arrows). Microtubules are in red (right) and were labeled with anti-tubulin antibody followed by rhodamine-labeled secondary antibody. Bars = 1 μm.

(C) and **(D)** Stereoimages of live protoplasts. MP:GFP is associated with the punctate structures connected by a fine cortical network with which MP:GFP is also associated. The strands between the periphery and interior of the cell are cytoplasmic streaming channels and known to contain ER. Bars = 10 μm.

(E) The cortical network with associated punctae (left) is similar to the reticulate pattern of the cortical ER that can be visualized after staining with $DIOC_6$ (right). Bars = 5 μm.

(F) The green fluorescent MP:GFP–associated cortical network (left) can be stained with antibody against ER-luminal BiP (center, red). Merging the MP:GFP (left) and BiP (center) signals produced a yellow color (right) indicating colocalization of MP:GFP and BiP to the cortical ER network. The punctate structures associated with the ER network were not stained by BiP antibody and thus may not be connected to the ER lumen. Bar = 5 μm.

(G) Effect of BFA, oryzalin, and Cyt D on MP:GFP accumulation at peripheral punctate structures. A nontreated protoplast showing fluorescent punctate structures of normal size, fluorescence, and distribution is shown at left. BFA inhibited accumulation of MP:GFP in punctate structures (center left). Oryzalin did not inhibit MP:GFP accumulation in the punctate structures. However, the punctate structures were noticeably larger than in nontreated protoplasts (center right). Cyt D caused reduced accumulation of MP:GFP in the punctate structures (right). Bars = 10 μm.

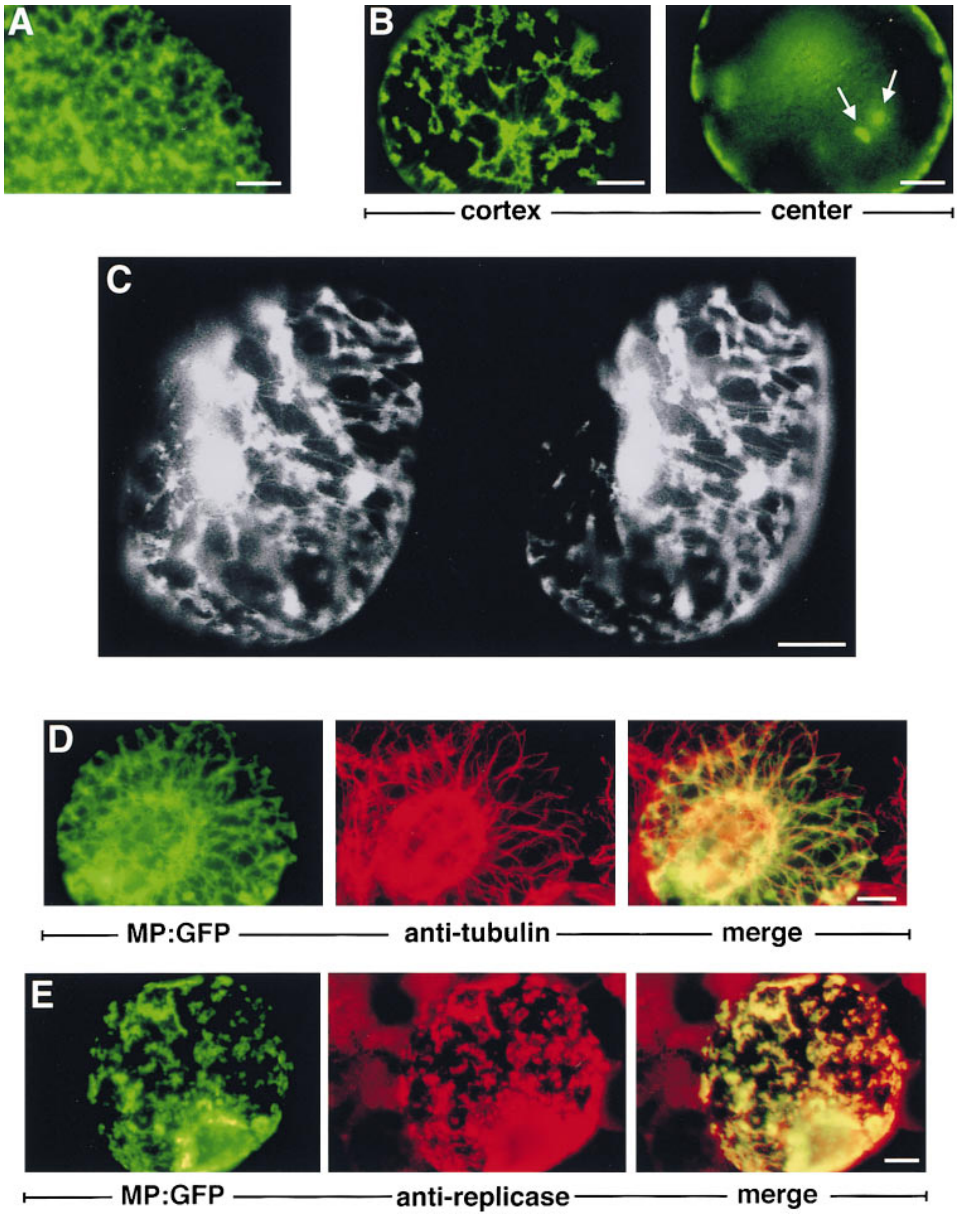

Figure 5. Irregular Fluorescent Structures Are Derived from the Cortical ER Associated with Microtubules and Contain TMV Replicase.

(A) The irregular fluorescent structures derive from local accumulations of MP:GFP at the cortical network early in infection. Bar = 5 μm.
(B) Live protoplast focused on the cortex (left) and center (right). Most of the irregularly shaped fluorescent structures occur in the outermost periphery of the protoplasts; only a few of these structures occur in the inner cytoplasm (arrows). Bars = 10 μm.
(C) Stereoimage showing irregular fluorescent bodies located immediately interior to microtubules. Bar = 10 μm.
(D) Irregular fluorescent structures are associated with microtubules (left). Microtubules were stained with anti-tubulin antibody and rhodamine-conjugated secondary antibody. Later during infection, the microtubules appear to redistribute MP:GFP from the irregular fluorescent structures (center). During this stage of infection, microtubules were associated with MP:GFP and also with membranes carrying the fusion protein (right). Bar = 10 μm.
(E) MP:GFP and replicase colocalize to the irregular structures. Bar = 10 μm.

stained with anti-actin or anti-tubulin antibodies and were formed in the presence of the cytoskeleton-disruptive agents Cyt D and oryzalin (data not shown).

Transient Expression of the MP

To determine whether targeting of MP and MP:GFP requires virus infection, protoplasts were transfected with plasmid p35S-MP or plasmid p35S-MP:GFP, which led to the transient production of MP and MP:GFP fusion protein, respectively. In these experiments, MP was localized to microtubules, punctate structures, and the cortical ER (Figure 6). The larger fluorescent structures associated with virus infection were not observed in these experiments. It is not known whether this reflects the lack of association of MP:GFP with such structures in the absence of virus infection or the inability to visualize the structures by the methods used here. Nevertheless, these studies confirmed that the targeting of MP:GFP to certain sites in protoplasts is independent of virus infection.

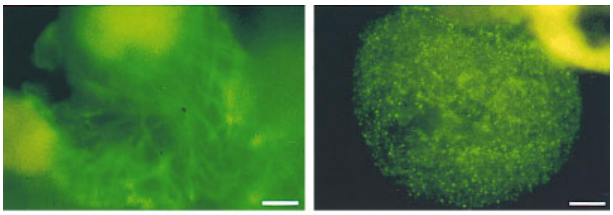

Figure 6. Transient Expression of MP or MP:GFP in Transfected Protoplasts.

Protoplasts were transfected with plasmid bearing the gene 35S-MP followed by antibody detection of the MP or with plasmid carrying the gene p35S-MP:GFP. Fluorescence distribution indicates localization of the MP (or MP:GFP) to microtubules (left) and to ER and associated punctate structures. Irregular fluorescent structures could not be detected. The occurrence of the nonfilamentous signal at left is due to low resolution of overlapping filaments. Bars = 10 μm.

DISCUSSION

Derivatives of TMV that express the MP as a fusion with the GFP were used to visualize the time course of MP accumulation and association with host components in infected *N. benthamiana* cells and BY-2 protoplasts. The subcellular locations of MP:GFP that we visualized by using fluorescence microscopy suggest the following temporal sequence of MP:GFP accumulation and distribution in infected protoplasts and leaves: MP:GFP first appeared (6 to 8 HPI) in peripheral punctate structures in protoplasts and in plasmodesmata in plants, where it persisted throughout infection. At ~12 HPI, the MP:GFP began to accumulate in irregularly shaped structures that derived from cortical ER. These fluorescent structures increased in size between 12 and 20 HPI and diminished thereafter as MP synthesis declined and the MP:GFP was redistributed onto microtubules. The association of MP:GFP with the irregular structures then diminished (starting at 16 HPI) and was associated with fluorescent microtubules together with peripheral punctate sites in protoplasts and with plasmodesmata in leaf cells. Finally, by ~30 HPI, the fluorescence on microtubules disappeared, and fluorescence was again confined to the punctate sites and protrusions appearing on the plasma membrane surface. At late stages of infection, we also observed a general haze of fluorescence throughout the cytosol that may represent free or partially degraded MP:GFP or modified soluble MP:GFP.

The amount of MP:GFP produced was less in cells infected by the virus construct that contained the CP open reading frame (TMV–MP:GFP–CP) than in cells infected with virus without the CP sequence, and it was increased by adding Act D to the culture medium. Because the fluorescent irregular structures occur during virus infection and contain replicase, we propose that they represent "viral factories," that is, sites at which virus replication and synthesis and accumulation of MP:GFP are concurrent. The finding that viral protein synthesis and virus replication occur in the same complex (Beachy and Zaitlin, 1975) may explain the observation that overexpression of MP:GFP in the presence of Act D resulted in its accumulation predominantly in the irregular fluorescent structures rather than at other sites of the cell. The fact that it was difficult to detect MP:GFP in the sites of virus replication in cells infected with TMV–MP:GFP–CP is consistent with reduced production of MP:GFP by this construct.

Von Wettstein and Zech (1962) reported that in leaves infected by TMV, large deposits of fibrous material were found on the cytoplasmic face of the ER that consisted of extensive folds of membrane. Our data indicate that TMV replicase is associated with the ER, particularly the cortical ER, and that the fluorescent irregular structures that contain replicase are derived from cortical ER. We suggest that the structures may be similar to those described in the earlier studies. This proposal is consistent with previous observations that the replication complexes of TMV copurify with membrane extracts from infected cells (Watanabe and Okada, 1986; Young and Zaitlin, 1986; Young et al., 1987; Restrepo et al., 1990; Osman and Buck, 1996). Recent experiments in our laboratory have confirmed that both the MP and replicase are associated with the ER isolated from infected leaf tissues (C. Reichel and R.N. Beachy, unpublished data). Other investigators have demonstrated that accumulation of replication proteins or nascent viral RNA synthesis of tobacco etch potyvirus (Schaad et al., 1997) and brome mosaic bromovirus (Restrepo-Hartwig and Ahlquist, 1996) occurs on the ER network, which, upon

infection, collapses into "discrete aggregated structures" or "cytoplasmic patches."

In cell fractionation studies, the TMV MP behaved as a highly hydrophobic protein and copurified with membranes that contain enzyme markers common to the ER (Moore et al., 1992; Fenczik, 1994). However, MP lacks an apparent ER signal sequence (Atkins et al., 1991b; Deom et al., 1991), and in in vitro translation reactions, it does not associate with dog pancreas membranes (C.M. Deom, T. Kahn, and R.N. Beachy, unpublished results). This raises the possibility that the MP does not enter the ER but rather interacts with the cytoplasmic face of the ER per se or with the endomembrane sheath of cytoskeleton and cytoskeleton-associated molecules that cloak the ER (Reuzeau et al., 1997a, 1997b). Together, these observations support the hypothesis that upon entry into a newly infected cell, MP and/or replicase attach to the cytoplasmic face of the membrane to establish a site of virus replication. ER-associated virus replication and accumulation of viral proteins occur concomitantly with membrane proliferation and give rise to the irregular fluorescent structures that are likely to be related to the "viroplasms" or "X-bodies" that were previously described (Shalla, 1964; Kohlemainen et al., 1965; Milne, 1966; Esau and Cronshaw, 1967a, 1967b) and contain viral replicase (Hills et al., 1987). The disappearance of MP from the viroplasm suggests that with the "maturation" of the viroplasm, MP synthesis is halted and/or MP is eliminated from the viroplasm and targeted for other sites in the cell or is degraded.

MP:GFP accumulates in punctate structures in protoplasts when expressed transiently from a constitutive promoter, and MP accumulates in plasmodesmata in transgenic plants (Ding et al., 1992; Moore et al., 1992). This supports the hypothesis that targeting of MP to plasmodesmata and punctate structures is an intrinsic property of the MP and does not require virus infection. The fluorescent punctate structures are located at or near the vertices of cortical ER. Oparka et al. (1994) described the cortical ER as being in proximity to the cell membrane at two kinds of sites (Oparka et al., 1994): one is at plasmodesmata, and one is independent of plasmodesmata. It is suggested that these sites have a number of features in common (Pickard, 1994).

The peripheral punctae are often regularly spaced and in some cells appear coincident with microtubules. It was previously postulated that microtubules attach at punctate cytoskeleton-to-membrane-to-wall adhesion sites in plant cells (Pickard and Ding, 1993). In our studies, we found that the fluorescent punctate sites swell or enlarge when microtubules are disrupted by oryzalin. This feature has also been described for sites at which the cortical ER and the overlying plasma membrane are anchored to the cell wall (Knebel et al., 1990; Lichtscheidl and Url, 1990); these sites are called cell wall adhesion sites or plasmalemmal control centers (Gens et al., 1996; Reuzeau et al., 1997a, 1997b).

Although Cyt D had no effect on the structure and distribution of the fluorescent punctate structures, it reduced their fluorescence, suggesting that filamentous actin plays a role in targeting or anchoring of the MP:GFP at these sites. In onion cells, actin is known to localize to putative cell wall adhesion sites and to be associated with the endomembrane sheath that clads the ER (Reuzeau et al., 1997a, 1997b). Actin also colocalizes with plasmodesmata (White et al., 1994; Ding and Kwon, 1996). Considering that actin confers structural stability and motor force to the ER (Allen and Brown, 1988; Karchar and Reese, 1988; Quader et al., 1989; Lichtscheidl et al., 1990), it is possible that F-actin mediates the association of the MP:GFP with appropriate regions of the ER and has a functional role in transporting the MP to plasmodesmata, as previously proposed (McLean et al., 1995; Zambryski, 1995).

Because accumulation of the MP:GFP in the punctate sites is not affected by treatment with oryzalin, microtubules may not have an immediate role in targeting the MP to these sites or, by inference, to the plasmodesmata. However, the proximity sometimes observed between the ER and microtubules (Lancelle et al., 1987; Hepler et al., 1990) and the observations that indicate that MP:GFP moves from the replicase-containing irregular fluorescent structures onto microtubules may suggest that microtubules are involved in propagating infection sites within the cell and providing an efficient subcellular long-distance transport system for translocation of the MP or viral complexes between infection sites and from these to (distant) plasmodesmata. It is also possible that microtubules participate in the degradation of the MP:GFP, as suggested by Padgett et al. (1996).

The appearance of MP:GFP plasma membrane protrusions is reminiscent of the projections on the surface of plant protoplasts and insect cells that express the movement proteins of tubule-forming viruses such as cowpea mosaic virus (van Lent et al., 1991; Wellink et al., 1993; Kasteel et al., 1996), cauliflower mosaic virus (Perbal et al., 1993; Kasteel et al., 1996), tomato spotted wilt virus (Storms et al., 1995), and grapevine fanleaf nepovirus (Ritzenthaler et al., 1995). In contrast to TMV, these viruses apparently move between cells as virions through such tubules. We suggest the possibility that the "hairs" reflect a tubule-forming function of the MP that generally is not observed in infected leaves. Alternatively, the capacity to form such structures may be a function of the MP that is not needed for infection of tobacco plants but is required in other hosts.

Taken together, our observations that the MP and the replicase are localized on the ER suggest a major role for the ER in viral pathogenesis. We propose that the MP and replicase are colocalized in complexes on the cytoplasmic face of the ER and give rise to viral factories that, in mature infections, form X-bodies. The actin cytoskeleton that clads the ER and confers structural stability as well as motor force may play a role in delivering and attaching the MP to the putative cell wall adhesion sites and the plasmodesmata. Microtubules may provide the major skeletal element that distributes viral replication complexes throughout the cell, for long-distance transport of the MP and the viral genome, and possibly for targeting the MP for degradation.

METHODS

Plasmids

The plasmids pTMV-M:GfusBr and pT-MfCP served as templates for production of infectious RNA of the viruses TMV-M:GfusBr and TMV-MfCP and were constructed as previously described (Oparka et al., 1997). For simplicity, we refer to TMV-M:GfusBr as TMV–MP:GFP, and TMV-MfCP as TMV–MP:GFP–CP. Both viruses encode the movement protein (MP) fused to the green fluorescent protein (GFP) that contains threonine in place of serine at amino acid position 65 (Heim et al., 1995) to increase brightness. The plasmid pU3/12 (Holt and Beachy, 1991) was used to generate infectious RNA of wild-type tobacco mosaic virus (TMV) (strain U1). Plasmid p35S-MP was generated by placement of the NdeI-AflII fragment containing the MP open reading frame from pT3′NA (Deom et al., 1994) into the EcoRI site of pMON999, a pUC-based plant expression cassette that includes the E35S promoter (Kay et al., 1987) and the nopaline synthase gene 3′ end. Plasmid p35S-MP:GFP was created by replacing the BsmBI-KpnI fragment of p35S-MP containing the 3′ terminus of the MP gene with the BsmBI-KpnI fragment of pTMV-M:GfusBr; the latter contains the same sequence of the MP gene fused to the GFP sequence and the 3′ end of TMV.

Inoculation of Plants and Protoplasts and Treatments with Inhibitors

Nicotiana benthamiana plants were mechanically inoculated by rubbing the leaves (in the presence of carborundum) with transcripts derived from in vitro reactions, and the plants were maintained at 23°C with a 14-hr photoperiod. Protoplasts of tobacco suspension cell line BY-2 were prepared and inoculated by electroporation with infectious transcripts, as described by Watanabe et al. (1982). After inoculation, protoplasts were resuspended in 10 mL of medium, and 1-mL aliquots in 35-mm Petri dishes were cultured in the dark at 28°C. Actinomycin D (Act D; 30 μg/mL), oryzalin (10 μM), cytochalasin D (Cyt D; 25 μg/mL), and brefeldin A (BFA; 50 μg/mL), where indicated, were added to the protoplasts from stock solutions prepared with DMSO as solvent. The presence of DMSO (0.1% [v/v]) in the culture medium had no effect on the results presented here. Act D, Cyt D, and BFA were purchased from Calbiochem (La Jolla, CA), and oryzalin was purchased from ChemService Inc. (West Chester, PA).

Fluorometric Analysis

Fluorometric analysis was performed with protoplasts inoculated with TMV-M:GfusBr, TMV-MfCP, or TMV-U1. For each virus, seven aliquots of 2×10^6 protoplasts were inoculated by electroporation, pooled, suspended in 70 mL of culture medium, and then divided into 1-mL aliquots for culturing. To half of each sample, Act D was added to a concentration of 30 μg/mL. Before fluorometric measurements, groups of five 1-mL aliquots of cells infected with the particular virus (and cultured either with or without Act D, respectively) were combined, and a 1-mL aliquot was retained for in situ analysis. Fluorescence emission was determined at 508 and 620 nm by using a spectrofluorometer (model RF 1501; Shimadzu, Kyoto, Japan) with excitation at 475 nm. The values obtained at 508 nm were divided by the value obtained at 620 nm to correct for possible differences in the number of protoplasts between the samples. The resulting E508/E620 values of protoplasts infected with TMV-U1 were subtracted from the E508/E620 values of the protoplasts infected with TMV-M:GfusBr and TMV-MfCP to correct for background fluorescence. Finally, each value was corrected for the ratio of infected (fluorescent) cells to total cells in the sample.

Immunofluorescent Labeling and Microscopy

Fixation and immunostaining of protoplasts were performed as described previously (Heinlein et al., 1995). Monoclonal mouse anti–α-tubulin antibodies were from Amersham (Arlington Heights, IL), monoclonal mouse anti-actin antibodies were from ICN (Costa Mesa, CA), and all fluorochrome-labeled secondary antibodies were from Pierce (Rockford, IL). Antibodies raised against the maize immunoglobulin binding protein (BiP) were kindly provided by R.S. Boston (North Carolina State University, Raleigh). Regular fluorescence microscopy was as described by Heinlein et al. (1995), and stereopair fluorescence photographs of live cells were taken with the Edge True-View 3D Head (Edge Scientific Instrument Company, Santa Monica, CA).

For $DiOC_6$ staining, protoplasts were incubated in 0.4 M mannitol containing 0.25% glutaraldehyde (Terasaki et al., 1984) and 5 μg/mL $DiOC_6$ (Molecular Probes, Eugene, OR) and observed immediately. Fluorescence images were scanned from 35-mm slides taken with Kodak Ektachrome 1600 EPH film and were arranged using Adobe Photoshop software (Adobe Systems Inc., Mountain View, CA).

Wide-Field Computational Optical-Sectioning Microscopy

The microscope, data acquisition system, and method of image restoration have been described elsewhere (Gens et al., 1996). A ×60, 1.4 NA Plan Apo lens was used (Nikon, Garden City, NY). The 6.8-μm CCD camera wells were binned 2 × 2, and the sectioning lens was moved in 0.45-μm increments so that voxel dimensions were X = Y = 0.22 μm and Z = 0.45 μm. The images were restored using the maximum likelihood algorithm, with 1000 iterations, and blur was removed by Gaussian filtering. Stereopairs were created from the three-dimensional images by displacing optical sections along rays angled 9° left and 9° right from the Z-axis, as appropriate for the voxel dimensions.

ACKNOWLEDGMENTS

We thank Linda Wagner at Edge Scientific Instrument Co. (Santa Monica, CA) for providing the Edge True-View 3D™ Head and Dr. Rebecca S. Boston (North Carolina State University, Raleigh) for providing anti–maize b-70 (BiP) antibody. This research was supported by the National Science Foundation (NSF) through Grants No. MCB 9317368 and No. MCB 9631124 to R.N.B.; by a grant from the United States of America–Israel Bi-National Agricultural Research and Development Fund (BARD) to R.N.B. and B.L.E.; by a National Aeronautics and Space Administration/NSF Joint Program in Plant Biology through Grant No. IBN941601 to B.G.P.; and by the Human

Frontier Science Program Organization through a long-term fellowship to M.H. J.S.G. was supported by a Monsanto Predoctoral Fellowship in Plant Biology. We thank Dr. James G. McNally for collegial support of optical sectioning microscopy activities.

Received February 23, 1998; accepted April 28, 1998.

REFERENCES

Allen, N.S., and Brown, D.T. (1988). Dynamics of the endoplasmic reticulum in living onion epidermal cells in relation to microtubules, microfilaments and intracellular particle movement. Cell Motil. Cytoskeleton **10,** 153–163.

Atkins, D., Roberts, K., Hull, R., Prehaud, C., and Bishop, D.H.L. (1991a). Expression of the tobacco mosaic virus movement protein using a baculovirus expression vector. J. Gen. Virol. **72,** 2831–2835.

Atkins, D., Hull, R., Wells, B., Roberts, K., Moore, P., and Beachy, R.N. (1991b). The tobacco mosaic virus 30K movement protein in transgenic tobacco plants is localized to plasmodesmata. J. Gen. Virol. **72,** 209–211.

Beachy, R.N., and Zaitlin, M. (1975). Replication of tobacco mosaic virus. VI. Replicative intermediate and other viral related RNAs associated with polyribosomes. Virology **63,** 84–97.

Blum, H., Gross, H.J., and Beier, H. (1989). The expression of the TMV-specific 30-kDa protein in tobacco protoplasts is strongly and selectively enhanced by actinomycin. Virology **169,** 51–61.

Boston, R.S., Viitanen, P.V., and Vierling, E. (1996). Molecular chaperones and protein folding in plants. Plant Mol. Biol. **32,** 191–222.

Carrington, J.C., Kasschau, K.D., Mahajan, S.K., and Schaad, M.C. (1996). Cell-to-cell and long-distance transport of viruses in plants. Plant Cell **8,** 1669–1681.

Citovsky, V., Knorr, D., Schuster, G., and Zambryski, P. (1990). The P30 movement protein of tobacco mosaic virus is a single-strand nucleic acid binding protein. Cell **60,** 637–647.

Citovsky, V., Wong, M.L., Shaw, A.L., Prasad, B.V.V., and Zambryski, P. (1992). Visualization and characterization of tobacco mosaic virus movement protein binding to single-stranded nucleic acids. Plant Cell **4,** 397–411.

Cole, N.B., and Lippincott-Schwartz, J. (1995). Organization of organelles and membrane traffic by microtubules. Curr. Opin. Cell Biol. **7,** 55–64.

Culver, J.N., Lehto, K., Close, S.M., Hilf, M.E., and Dawson, W.O. (1993). Genomic position affects the expression of tobacco mosaic virus movement and coat protein genes. Proc. Natl. Acad. Sci. USA **90,** 2055–2059.

Deom, C.M., Oliver, M.J., and Beachy, R.N. (1987). The 30-kilodalton gene product of tobacco mosaic virus potentiates virus movement. Science **237,** 389–394.

Deom, C.M., Wolf, S., Holt, C.A., Lucas, W.J., and Beachy, R.N. (1991). Altered function of the tobacco mosaic virus movement protein in a hypersensitive host. Virology **180,** 251–256.

Deom, C.M., Xian, Z.H., Beachy, R.N., and Weissinger, A.K. (1994). Influence of heterologous tobamovirus movement protein and chimeric-movement protein genes on cell-to-cell and long-distance movement. Virology **205,** 198–209.

Ding, B., and Kwon, M.-O. (1996). Evidence that actin filaments are involved in controlling the permeability of plasmodesmata in tobacco mesophyll. Plant J. **10,** 157–164.

Ding, B., Haudenshield, J.S., Hull, R.J., Wolf, S., Beachy, R.N., and Lucas, W.J. (1992). Secondary plasmodesmata are specific sites of localization of the tobacco mosaic virus movement protein in transgenic tobacco plants. Plant Cell **4,** 915–928.

Driouich, A., Zhang, G.F., and Staehelin, A.L. (1993). Effect of brefeldin A on the structure of the Golgi apparatus and on the synthesis and secretion of proteins and polysaccharides in sycamore maple (*Acer pseudoplatanus*) suspension-cultured cells. Plant Physiol. **101,** 1363–1373.

Epel, B.L. (1994). Plasmodesmata: Composition, structure and trafficking. Plant Mol. Biol. **26,** 1343–1356.

Epel, B.L., Padgett, H.S., Heinlein, M., and Beachy, R.N. (1996). Plant virus movement protein dynamics probed with a GFP–protein fusion. Gene **173,** 75–79.

Esau, K., and Cronshaw, J. (1967a). Relation of tobacco mosaic virus to the host cells. J. Cell Biol. **33,** 665–678.

Esau, K., and Cronshaw, J. (1967b). Tubular components in cells of healthy and tobacco mosaic virus–infected *Nicotiana.* Virology **33,** 26–35.

Fenczik, C.A. (1994). Characterization of Two Tobamoviruses: Movement Proteins and Their Role in Host Range Determination. PhD Dissertation (St. Louis, MO: Washington University).

Fenczik, C.A., Epel, B.L., and Beachy, R.N. (1995). Role of plasmodesmata and virus movement proteins in spread of plant viruses. In Signal Transduction in Plant Growth and Development, D.P.S. Verma, ed (New York: Springer-Verlag), pp. 249–272.

Fontes, E.B.P., Shank, B.B., Wrobel, R.L., Moose, S.P., OBrian, G.R., Wurtzel, E.T., and Boston, R.S. (1991). Characterization of an immunoglobulin binding protein homolog in the maize *floury-2* endosperm mutant. Plant Cell **3,** 483–496.

Gens, J.S., Reuzeau, C., Doolittle, K.W., McNally, J.G., and Pickard, B.G. (1996). Covisualization by computational optical-sectioning microscopy of an array of integrin and associated proteins at the cell membrane of living onion protoplasts. Protoplasma **194,** 215–230.

Heim, R., Cubitt, A.B., and Tsien, R.Y. (1995). Improved green fluorescence. Nature **373,** 663–664.

Heinlein, M., Epel, B.L., Padgett, H.S., and Beachy, R.N. (1995). Interaction of tobamovirus movement proteins with the plant cytoskeleton. Science **270,** 1983–1985.

Henderson, J., Satiat-Jeunemaitre, B., Napier, R., and Hawes, C. (1994). Brefeldin A–induced disassembly of the Golgi apparatus is followed by disruption of the endoplasmic reticulum in plant cells. J. Exp. Bot. **45,** 1347–1351.

Hepler, P.K., Palevitz, B.A., Lancelle, S.A., McCauley, M.M., and Lichtscheidl, I. (1990). Cortical endoplasmic reticulum in plants. J. Cell Sci. **96,** 355–373.

Hills, G.J., Plaskitt, K.A., Young, N.D., Dunigan, D.D., Watts, J.W., Wilson, T.M.A., and Zaitlin, M. (1987). Immunogold local-

ization of the intracellular sites of structural and nonstructural tobacco mosaic virus proteins. Virology **161,** 488–496.

Holt, C.A., and Beachy, R.N. (1991). *In vivo* complementation of infectious transcripts from mutant tobacco mosaic virus cDNAs in transgenic plants. Virology **181,** 109–117.

Hugdahl, J.D., and Morejohn, L.C. (1993). Rapid and reversible high-affinity binding of the dinitroaniline herbicide oryzalin to tubulin of *Zea mays* L. Plant Physiol. **102,** 725–740.

Johnston, S.S. (1995). The intracellular localization of messenger RNAs. Cell **81,** 161–170.

Karchar, B., and Reese, T.S. (1988). The mechanism of cytoplasmic streaming in characean algal cells: Sliding of endoplasmic reticulum along actin filaments. J. Cell Biol. **106,** 1545–1552.

Kasteel, D.T.J., Perbal, M.-C., Boyer, J.-C., Wellink, J., Goldbach, R.W., Maule, A.J., and van Lent, J.W.M. (1996). The movement proteins of cowpea mosaic virus and cauliflower mosaic virus induce tubular structures in plant and insect cells. J. Gen. Virol. **77,** 2857–2864.

Kay, R., Chan, A., Daly, M., and McPherson, J. (1987). Duplication of CaMV 35S promoter sequences creates a strong enhancer for plant genes. Science **236,** 1299–1302.

Knebel, W., Quader, H., and Schnepf, E. (1990). Mobile and immobile endoplasmic reticulum in onion bulk epidermis cells: Short- and long-term observations with a confocal laser scanning microscope. Eur. J. Cell Biol. **52,** 328–340.

Kohlemainen, I.H., Zech, H., and von Wettstein, D. (1965). The structure of cells during tobacco mosaic virus reproduction. Mesophyll cells containing virus crystals. J. Cell Biol. **25,** 77–97.

Lancelle, S.A., Cresti, M., and Hepler, P.K. (1987). Ultrastructure of the cytoskeleton in freeze-substituted pollen tubes of *Nicotiana alata.* Protoplasma **140,** 141–150.

Lichtscheidl, I.K., and Url, W.G. (1990). Organization and dynamics of cortical endoplasmic reticulum in inner epidermal cells of onion bulb scales. Protoplasma **157,** 203–215.

Lichtscheidl, I.K., Lancelle, S.A., and Hepler, P.K. (1990). Actin–endoplasmic reticulum complexes in *Drosera*: Their structural relationship with the plasmalemma, nuclei and organelles in cells prepared by high pressure freezing. Protoplasma **155,** 116–126.

Lucas, W.J., and Gilbertson, R.L. (1994). Plasmodesmata in relation to viral movement within leaf tissues. In Annual Review of Phytopathology, R.J. Cook, ed (Palo Alto, CA: Annual Reviews Inc.), pp. 387–412.

McLean, B.G., Zupan, J., and Zambryski, P.C. (1995). Tobacco mosaic virus movement protein associates with the cytoskeleton in tobacco cells. Plant Cell **7,** 2101–2114.

Meshi, T., Watanabe, Y., Saito, T., Sugimoto, A., Maeda, T., and Okada, Y. (1987). Function of the 30 kD protein of tobacco mosaic virus: Involvement in cell-to-cell movement and dispensability for replication. EMBO J. **6,** 2557–2563.

Milne, R.G. (1966). Multiplication of tobacco mosaic virus in tobacco leaf palisade cells. Virology **28,** 79–89.

Moore, P.J., Fenczik, C.A., and Beachy, R.N. (1992). Developmental changes in plasmodesmata in transgenic plants expressing the movement protein of tobacco mosaic virus. Protoplasma **170,** 115–127.

Nelson, R.S., Li, G., Hodgson, R.A.J., Beachy, R.N., and Shintaku, M.H. (1993). Impeded systemic accumulation of the masked strain of tobacco mosaic virus. Mol. Plant-Microbe Interact. **6,** 45–54.

Oparka, K.J., Prior, D.A.M., and Crawford, J.W. (1994). Behavior of plasma membrane, cortical ER and plasmodesmata during plasmolysis of onion epidermal cells. Plant Cell Environ. **17,** 163–171.

Oparka, K.J., Prior, D.A.M., Santa Cruz, S., Padgett, H.S., and Beachy, R.N. (1997). Gating of epidermal plasmodesmata is restricted to the leading edge of expanding infection sites of tobacco mosaic virus. Plant J. **12,** 781–789.

Osman, T.A., and Buck, K.W. (1996). Complete replication *in vitro* of tobacco mosaic virus RNA by a template-dependent, membrane-bound RNA polymerase. J. Virol. **70,** 6227–6234.

Padgett, H.S., Epel, B.L., Heinlein, M.H., Watanabe, Y., and Beachy, R.N. (1996). Distribution of tobamovirus movement protein in infected cells and implications for cell-to-cell spread of infection. Plant J. **10,** 1079–1099.

Perbal, M.-C., Thomas, C.L., and Maule, A.J. (1993). Cauliflower mosaic virus gene I product (P1) forms tubular structures which extend from the surface of infected protoplasts. Virology **195,** 281–285.

Pickard, B.G. (1994). Contemplating the plasmalemmal control center model. Protoplasma **182,** 1–9.

Pickard, B.G., and Ding, J.P. (1993). The mechanosensory calcium-selective ion channel: Key component of a plasmalemmal control center? Aust. J. Plant Physiol. **20,** 439–459.

Quader, H., Hoffman, A., and Schnepf, E. (1987). Shape and movement of the endoplasmic reticulum in onion bulb cells: Possible involvement of actin. Eur. J. Cell Biol. **44,** 17–26.

Quader, H., Hoffman, A., and Schnepf, E. (1989). Reorganization of the endoplasmic reticulum in epidermal cells of onion bulk scales after cold stress: Involvement of cytoskeletal elements. Planta **177,** 273–280.

Restrepo, M.A., Freed, D.D., and Carrington, J.C. (1990). Nuclear transport of plant potyviral proteins. Plant Cell **2,** 987–998.

Restrepo-Hartwig, M.A., and Ahlquist, P. (1996). Brome mosaic virus helicase- and polymerase-like proteins colocalize on the endoplasmic reticulum at sites of viral RNA synthesis. J. Virol. **70,** 8908–8916.

Reuzeau, C., Doolittle, K.W., McNally, J.G., and Pickard, B.G. (1997a). Covisualization in living onion cells of putative integrin, spectrin, actin, intermediate filaments and other proteins at the cell membrane and in an endomembrane sheath. Protoplasma **199,** 173–197.

Reuzeau, C., McNally, J.G., and Pickard, B.G. (1997b). The endomembrane sheath: A key structure for understanding the plant cell? Protoplasma **200,** 1–9.

Ritzenthaler, C.S., Michler, P., Stussi-Garaud, C., and Pinck, L. (1995). Grapevine fanleaf nepovirus putative movement protein is involved in tubule formation *in vivo.* Mol. Plant-Microbe Interact. **8,** 379–387.

Rutten, T.L.M., and Knuiman, B. (1993). Brefeldin A effects on tobacco pollen tubes. Eur. J. Cell Biol. **16,** 247–255.

Satiat-Jeunemaitre, B., and Hawes, C. (1993). Insights into the secretory pathways and vesicular transport in plant cells. Biol. Cell **79,** 7–15.

Satiat-Jeunemaitre, B., Cole, L., Bourett, T., Howard, R., and Hawes, C. (1996). Brefeldin A effects in plant and fungal cells: Something new about vesicle trafficking? J. Microsc. **181,** 162–177.

Schaad, M.C., Jensen, P.E., and Carrington, J.C. (1997). Formation of plant RNA virus replication complexes on membranes: Role of an endoplasmic reticulum–targeted viral protein. EMBO J. **16,** 4049–4059.

Schindler, T., Bergfeld, R., Hohl, M., and Schopfer, P. (1994). Inhibition of Golgi apparatus function by brefeldin A in maize coleoptiles and its consequences on auxin mediated growth, cell-wall extensibility, and secretion of cell wall proteins. Planta **192,** 404–413.

Shalla, T.A. (1964). Assembly and aggregation of tobacco mosaic virus in tomato leaflets. J. Cell Biol. **21,** 253–264.

Storms, M.M.H., Kormelink, R., Peters, D., van Lent, J.W.M., and Goldbach, R. (1995). The nonstructural NSM protein of tomato spotted wilt virus induces tubular structures in plant and insect cells. Virology **214,** 485–493.

Terasaki, M., Song, J., Wong, J.R., Weiss, M.J., and Chen, L.B. (1984). Localization of endoplasmic reticulum in living and glutaraldehyde-fixed cells with fluorescent dyes. Cell **38,** 101–108.

Tomenius, K., Clapham, D., and Meshi, T. (1987). Localization by immunogold cytochemistry of the virus-coded 30K protein in plasmodesmata of leaves infected with tobacco mosaic virus. Virology **160,** 363–371.

van Lent, J., Storms, M., Van der Meer, F., Wellink, J., and Goldbach, R. (1991). Tubular structures involved in movement of cowpea mosaic virus are also formed in infected cowpea protoplast. J. Gen. Virol. **72,** 2615–2623.

von Wettstein, D., and Zech, H. (1962). The structure of nucleus and cytoplasm in hair cells during tobacco mosaic virus reproduction. Z. Naturforsch. **17b,** 376–379.

Watanabe, Y., and Okada, Y. (1986). *In vitro* viral RNA synthesis by a subcellular fraction of TMV-inoculated tobacco protoplasts. Virology **149,** 73–74.

Watanabe, Y., Ohno, T., and Okada, Y. (1982). Virus multiplication in tobacco protoplasts inoculated with tobacco mosaic virus RNA encapsulated in large unilamellar vesicle liposomes. Virology **120,** 478–480.

Wellink, J., van Lent, J.W.M., Verver, J., Sijen, T., Goldbach, R.W., and Van Kammen, A. (1993). The cowpea mosaic M RNA-encoded 48-kilodalton protein is responsible for induction of tubular structures in protoplasts. J. Virol. **67,** 3660–3664.

White, R.G., Badett, K., Overall, R.L., and Vesk, M. (1994). Actin associated with plasmodesmata. Protoplasma **180,** 169–184.

Wilhelm, J.E., and Vale, R.D. (1993). RNA on the move: The mRNA localization pathway. J. Cell Biol. **123,** 269–274.

Wolf, S., Deom, C.M., Beachy, R.N., and Lucas, W.J. (1989). Movement protein of tobacco mosaic virus modifies plasmodesmatal size exclusion limit. Science **246,** 377–379.

Young, N.D., and Zaitlin, M. (1986). An analysis of tobacco mosaic virus replicative structures synthesized *in vitro.* Plant Mol. Biol. **6,** 455–465.

Young, N.D., Forney, J., and Zaitlin, M. (1987). Tobacco mosaic virus replicase and replicative structures. J. Cell Sci. **7** (suppl.), 277–285.

Zambryski, P. (1995). Plasmodesmata: Plant channels for molecules on the move. Science **270,** 1943–1944.